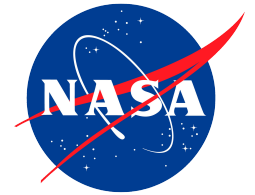




Meeting on QTN



Precision electron measurements in the solar wind: quasi thermal noise versus distribution functions by electrostatic analyzers

Chadi Salem, Marc Pulupa, Yuguang Tong & Stuart D. Bale

Space Sciences Laboratory, University of California, Berkeley, California, USA

Meudon, March 4-8, 2016

The different populations of the solar wind eVDFs

70 [Lin et al., 1998] R. P. LIN

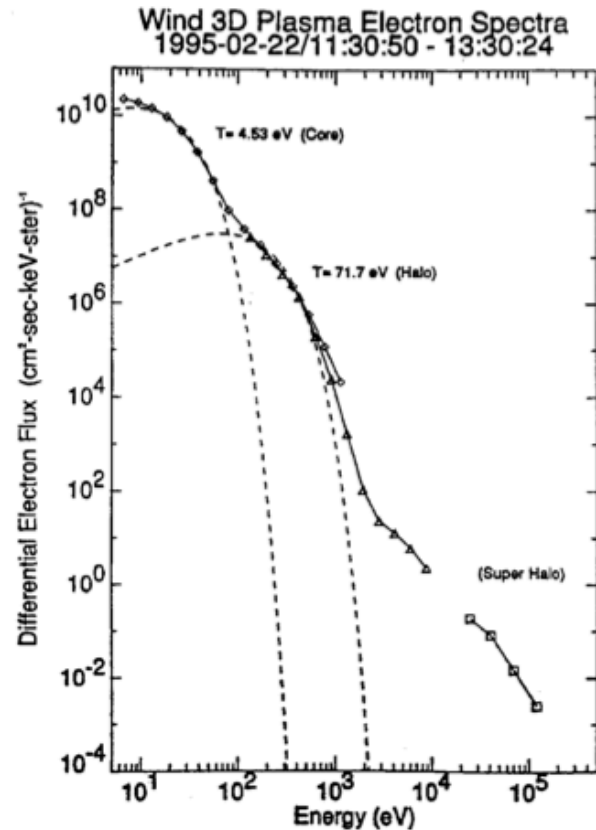
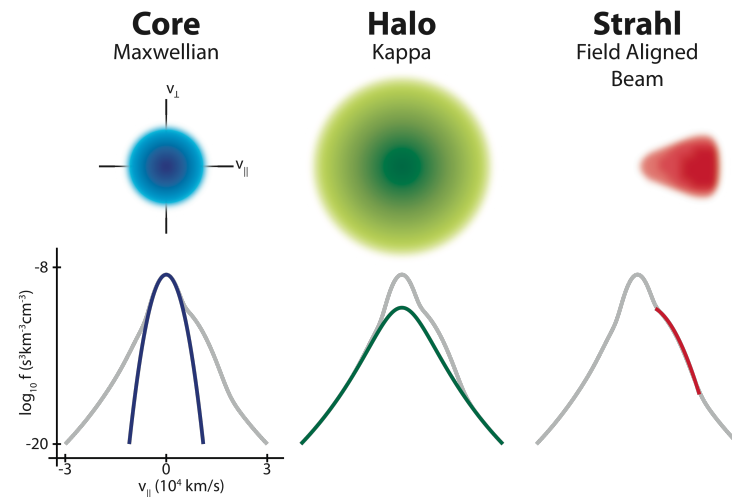


Figure 6. Electron differential flux spectrum from ~ 5 eV to $\gtrsim 100$ keV, measured at a very quiet time, in the absence of any solar particle events, by the WIND 3-D Plasma and Energetic Particle experiment. The diamonds, triangles, and squares indicate the three different detectors used to accommodate the wide range of fluxes over this energy range. The dashed lines give fits to Maxwellians for the solar wind core and halo.

- A thermal **core** population ($\sim 96\%$).
- A suprathermal **halo** and a field-aligned suprathermal **Strahl** propagating away from the Sun ($\sim 4\%$) [Pilipp et al., 1987]
- At even higher energies, up to 100 keV, a **super-halo** is observed in the ambient solar wind [Lin et al., 1998].



Our Work on Wind Measurements of Solar Wind Electrons

We developed a comprehensive code to get **Precision Electron Measurements** and to perform a detailed analysis of the structure in core-halo-strahl of the electron distribution functions (eVDFs).

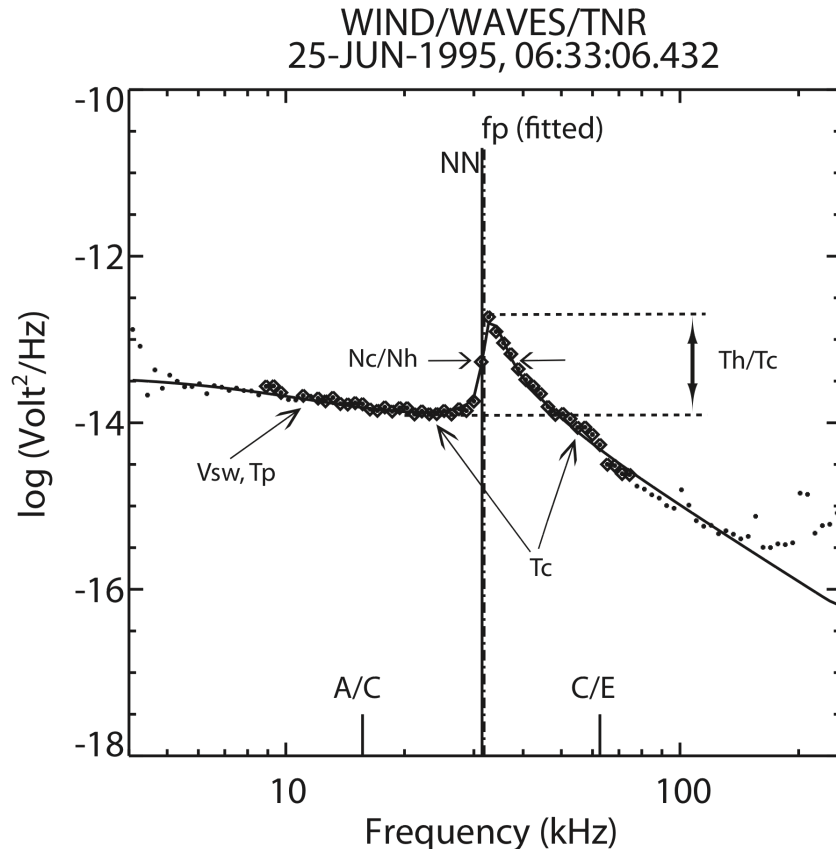
- Spacecraft potential determined [monopole spacecraft potential with Thermal Noise Measurements + dipole potential correction] and included in the processing of the eVDFs.
- EESA-L and EESA-H data are combined from a few eV to 2keV: Core and halo populations modeled by a bi-Maxwellian and a bi-Kappa distributions.
- Strahl population extracted and analyzed separately.
- Full sets of parameters for the core, halo and strahl populations computed.

⇒ This technique leads to a precise characterization of both thermal and suprathermal electron populations.

⇒ This technique is used to build an accurate database of solar wind electron parameters for the entire Wind mission.

Precision Electron Measurements & Thermal Noise Spectroscopy

[Meyer-Vernet & Perche, 1989; Issautier et al., 1999; Salem, 2000; Salem et al., 2001, 2003]

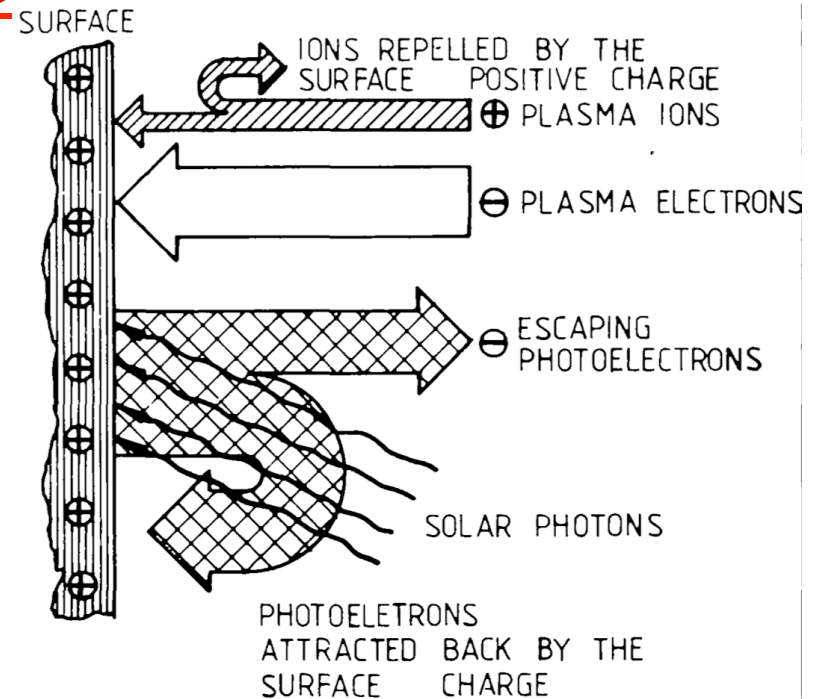


- The electric field spectrum around the electron plasma frequency contains a wealth of information about the solar wind electron populations: peak above f_{pe} determined by the eVDF.
- Theoretical spectrum uses a core-halo model of the eVDF.
- Fitting theoretical spectrum to observations $\Rightarrow N_e, T_c, N_h/N_c, T_h/T_c$, as well as V_{sw}, T_p
- Thermal noise is largely immune to spacecraft potential \Rightarrow TNR density used as a reference!

Use **quasi-thermal noise** (electric fluctuation) measurements to constrain the absolute plasma density – immune to s/c charging effects! Requires $L \gg \lambda_D$

Spacecraft Charging Effects

- In the solar wind, spacecraft charges slightly (a few eV) positive due to solar UV photoemission.
- Spacecraft potential distorts the thermal part of the eVDFs and affects parameters (N_e , T_e) measured by plasma instruments.
- Potential is dependent on N_e and T_e , which is what we want to measure!



[Grard et al., 1983]

Spacecraft potential determined first by finding the value needed for the (model) electron density to match the TNR density. This estimate is then compared to independent estimates obtained using a current balance model, taking into account the thermal and plasma drift velocity effects on the incoming ion and electron currents, and currents from photoelectron and secondary electron emissions.

Note: **1V ~ 600 km/s for an electron**

Core-Halo model of the eVDFs

Core = bi-Maxwellian and Halo = bi-Kappa

$$f(v_{\parallel}, v_{\perp}) = n_c \left(\frac{m}{2\pi} \right)^{3/2} \frac{1}{T_{c\perp} \sqrt{T_{c\parallel}}} \exp \left(-\frac{m}{2} \left(\frac{(v_{\perp} - v_{c\perp})^2}{T_{c\perp}} + \frac{(v_{\parallel} - v_{c\parallel})^2}{T_{c\parallel}} \right) \right) \\ + n_h \left(\frac{m}{\pi(2\kappa - 3)} \right)^{3/2} \frac{1}{T_{h\perp} \sqrt{T_{h\parallel}}} \frac{\Gamma(\kappa + 1)}{\Gamma(\kappa - 1/2)} \left(1 + \frac{m}{2\kappa - 3} \left(\frac{(v_{\perp} - v_{h\perp})^2}{T_{h\perp}} + \frac{(v_{\parallel} - v_{h\parallel})^2}{T_{h\parallel}} \right) \right)^{(-\kappa - 1)}$$

Fits are performed in the perpendicular direction first, then in the parallel direction using:

$$f(v) = A_0 \exp \left(-\frac{(v - A_1)^2}{A_2} \right) + A_3 \left(1 + \left(\frac{(v - A_4)^2}{A_5} \right)^{-A_6} \right)$$

$$P_{0\perp} = n_c = A_0 (2\pi/m)^{3/2} (A_{2\perp} A_{2\parallel}^{1/2})$$

$$P_{1\perp} = V_{c\perp} = A_{1\perp}$$

$$P_{2\perp} = T_{c\perp} = mA_{2\perp}/2$$

$$P_{3\perp} = n_h = A_3 \pi^{3/2} A_{5\perp} A_{5\parallel}^{1/2} \Gamma(A_6 - 3/2) / \Gamma(A_6)$$

$$P_{4\perp} = V_{h\perp} = A_{4\perp}$$

$$P_{5\perp} = T_{h\perp} = mA_{5\perp} / (2(A_6 - 1) - 3)$$

$$P_{6\perp} = \kappa = A_6 - 1$$

$$P_{0\parallel} = n_c = A_0 (2\pi/m)^{3/2} (A_{2\perp} A_{2\parallel}^{1/2})$$

$$P_{1\parallel} = V_{c\parallel} = A_{1\parallel}$$

$$P_{2\parallel} = T_{c\parallel} = mA_{2\parallel}/2$$

$$P_{3\parallel} = n_h = A_3 \pi^{3/2} A_{5\perp} A_{5\parallel}^{1/2} \Gamma(A_6 - 3/2) / \Gamma(A_6)$$

$$P_{4\parallel} = V_{h\parallel} = A_{4\parallel}$$

$$P_{5\parallel} = T_{h\parallel} = mA_{5\parallel} / (2(A_6 - 1) - 3)$$

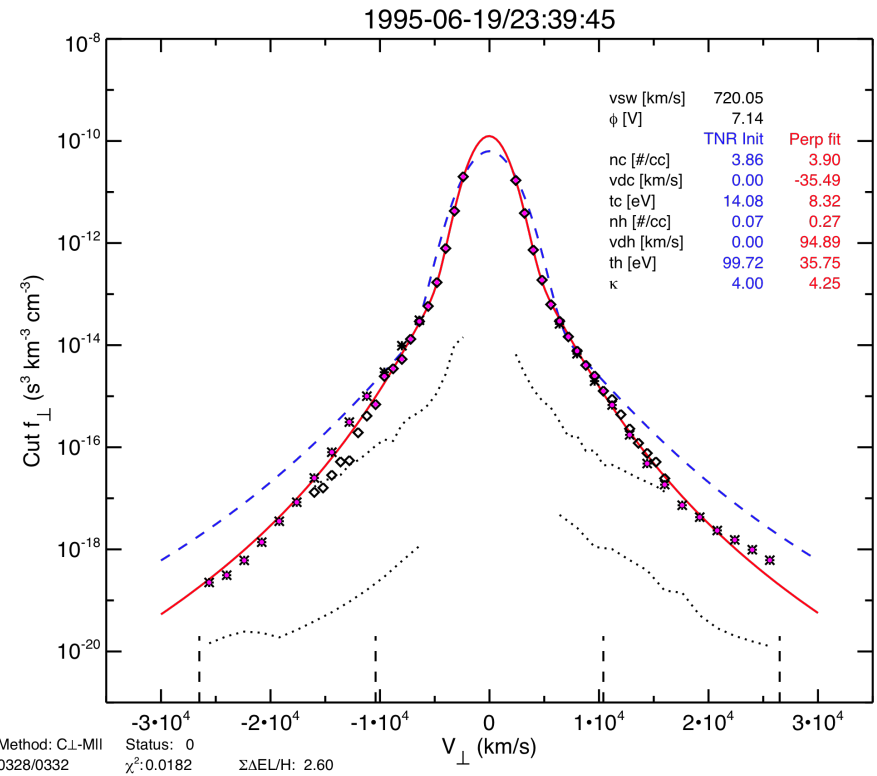
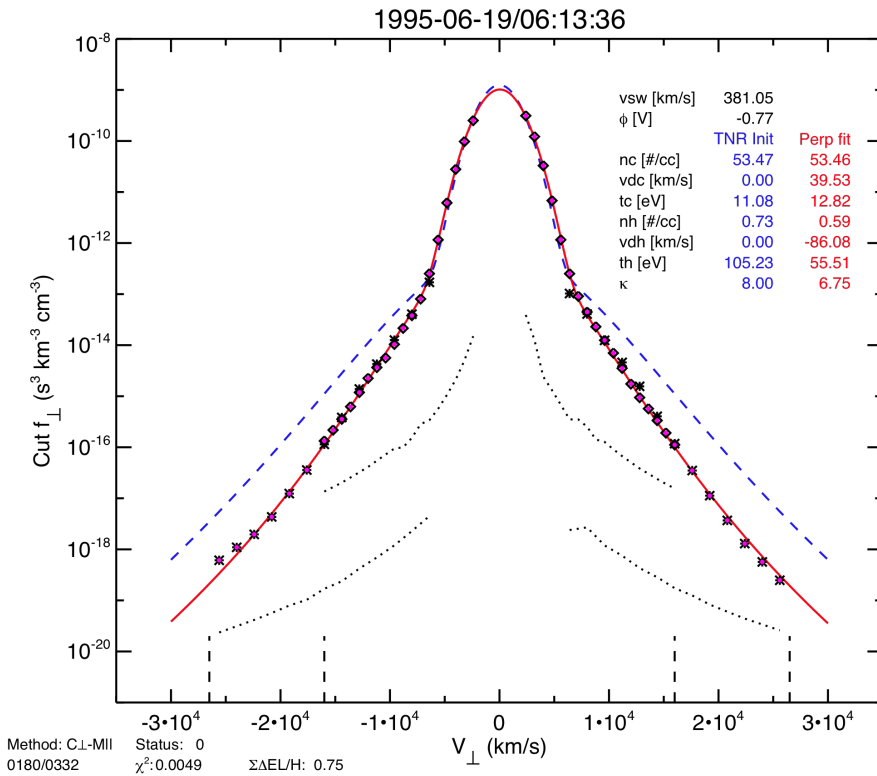
$$P_{6\parallel} = \kappa = A_6 - 1$$

WIND/3DP observations of eVDFs in the Solar Wind

Perpendicular cuts: core-halo fit, no strahl

Slow wind

Fast wind

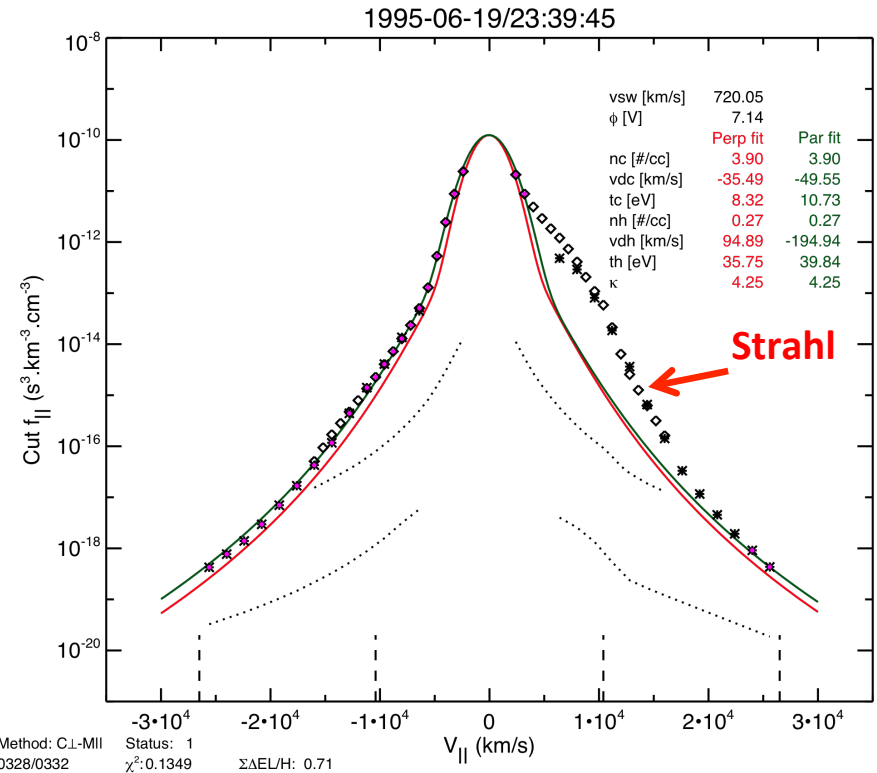
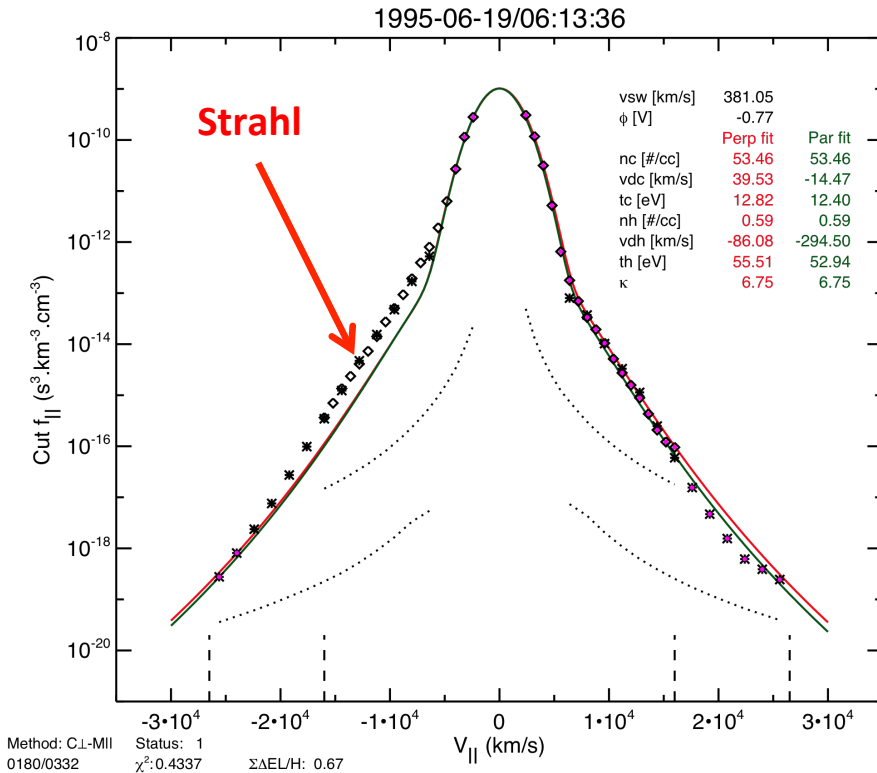


Red curve = fit by a sum of a Maxwellian and a Kappa to the perpendicular cut.

Parallel cuts: Core and halo fit, ignoring strahl points

Slow wind

Fast wind

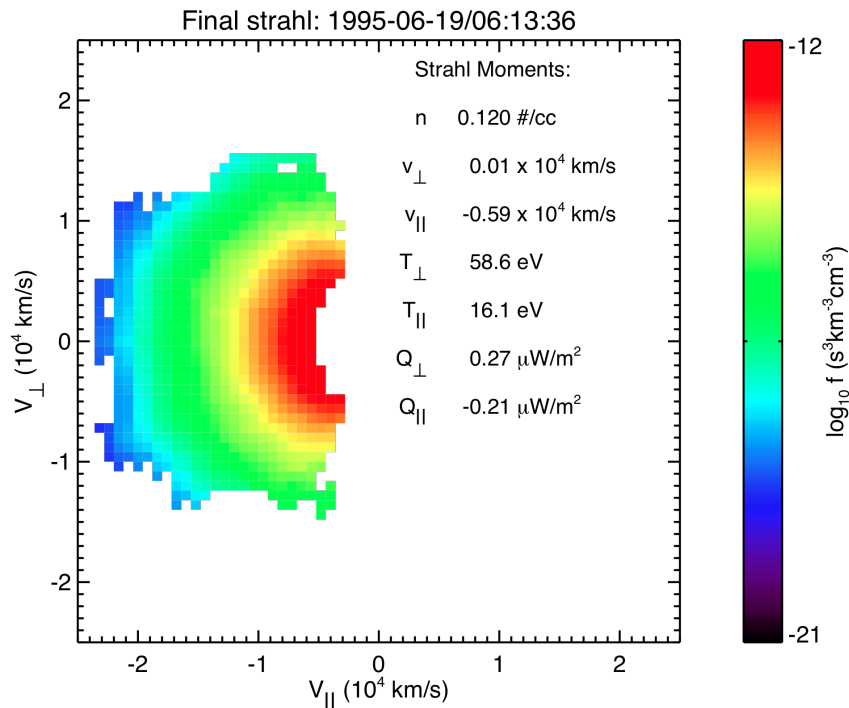


Green curve = fit by a sum of a Maxwellian and a Kappa to the parallel cut.
Red curve = perpendicular fit.

Extracting the Strahl Population

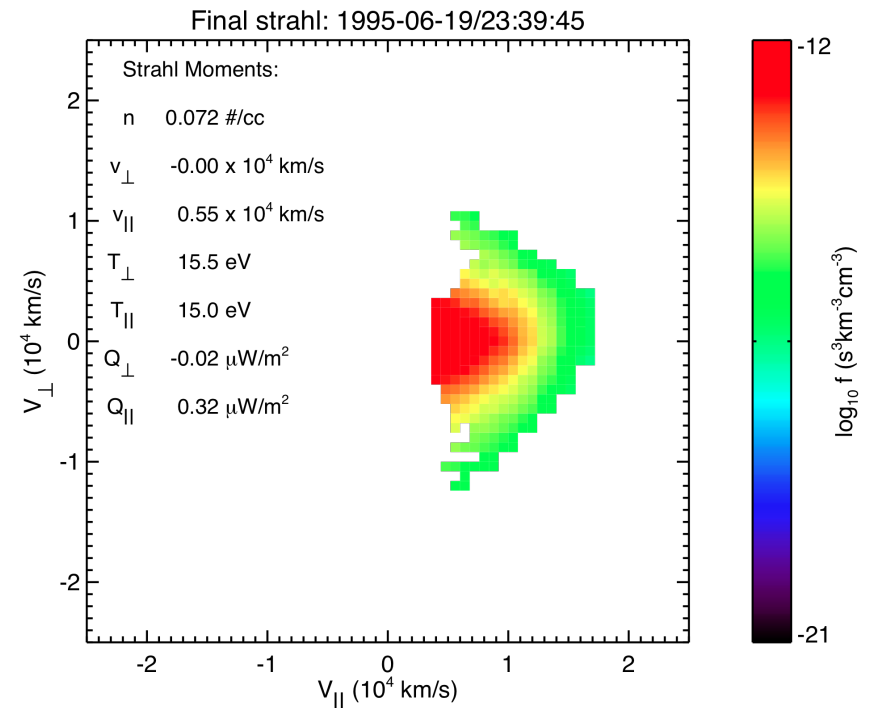
Representing $(f_{\text{data}} - f_{\text{model}})$ for $\Delta > 1$

Slow wind



0180/0332

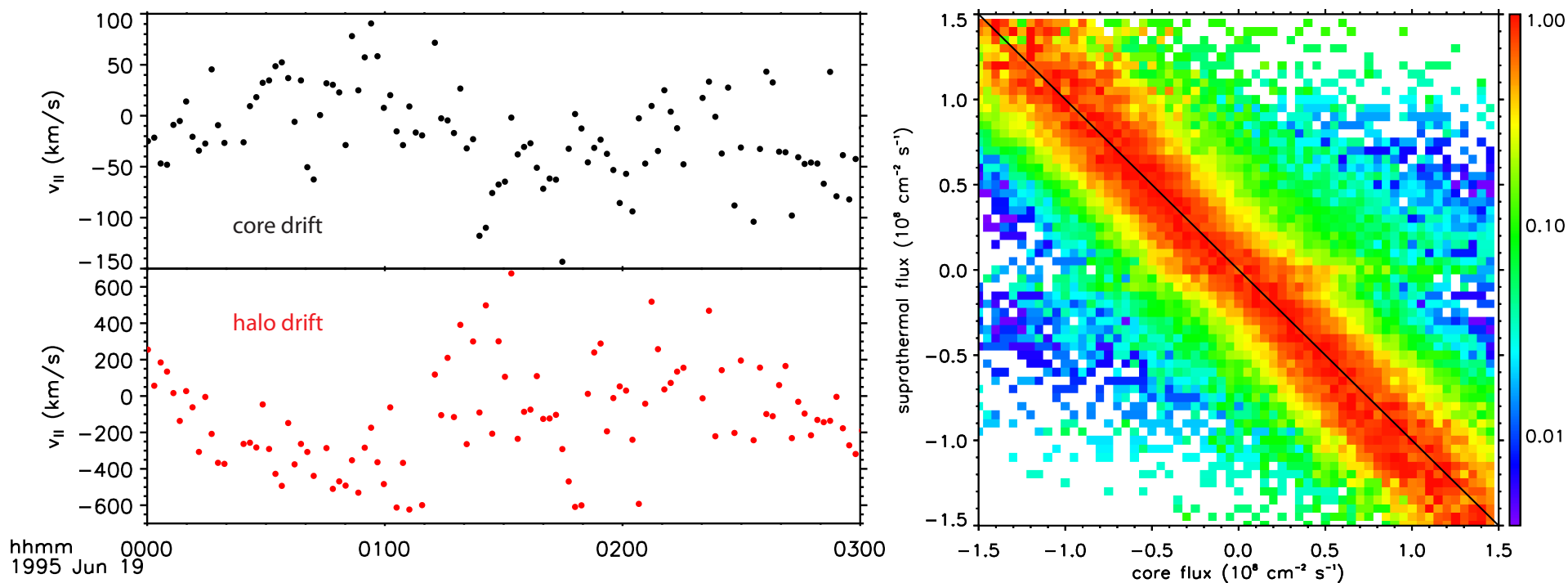
Fast wind



0328/0332

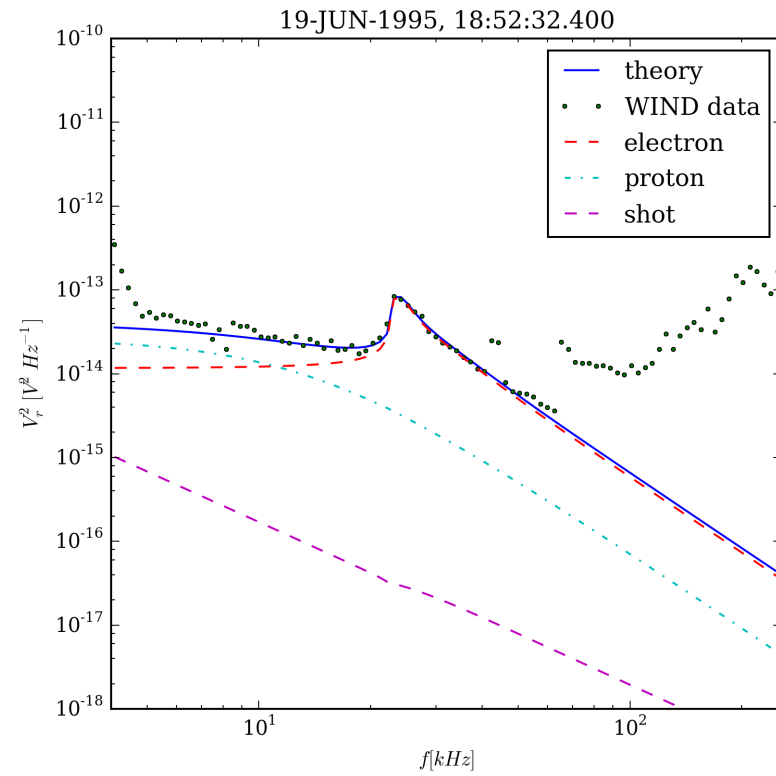
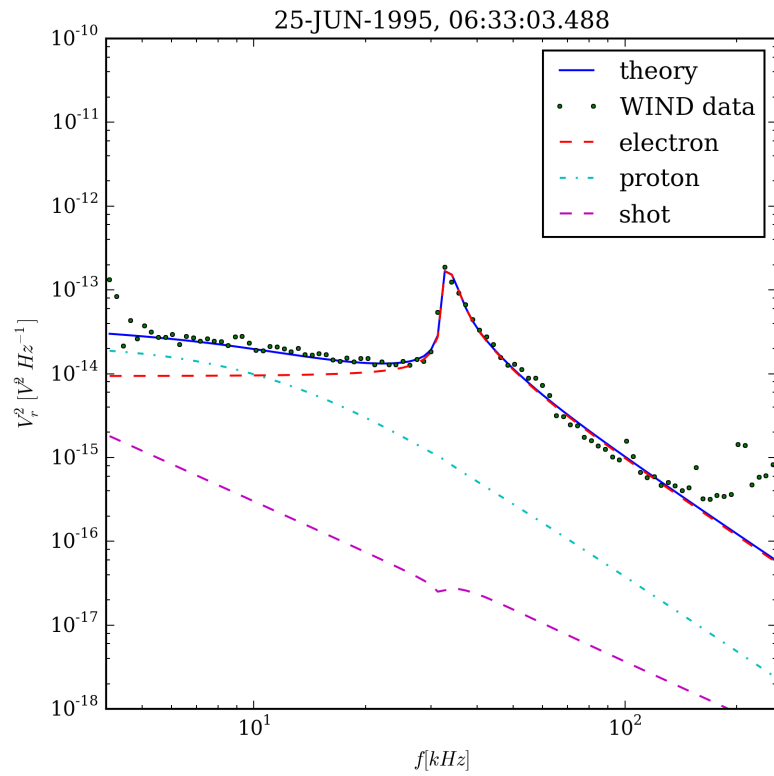
Final strahl can be analyzed for moments and parameterized

Current balance in the proton frame

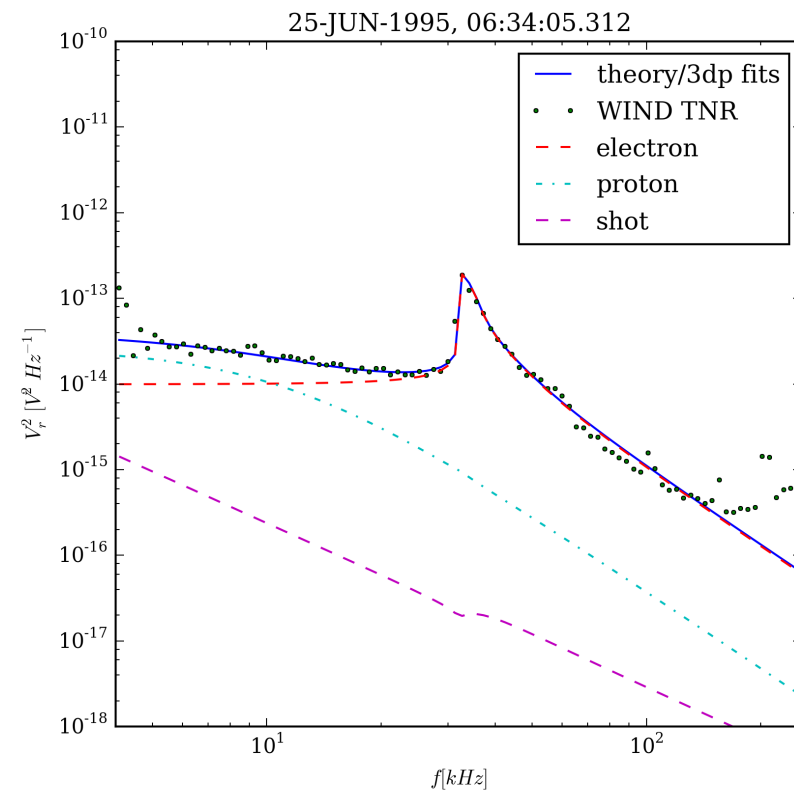
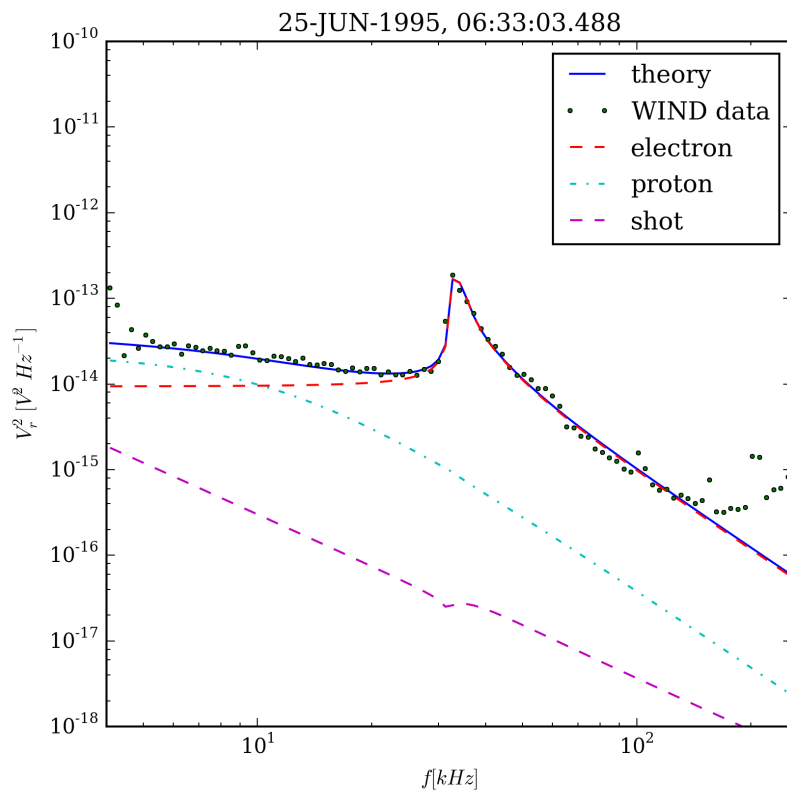


In the charge-center ($\sim \text{cm}$) frame, we expect zero net current: $n_c v_c + n_h v_h + n_s v_s = 0$, which seems to be so...

QTN with a sum of two Maxwellian

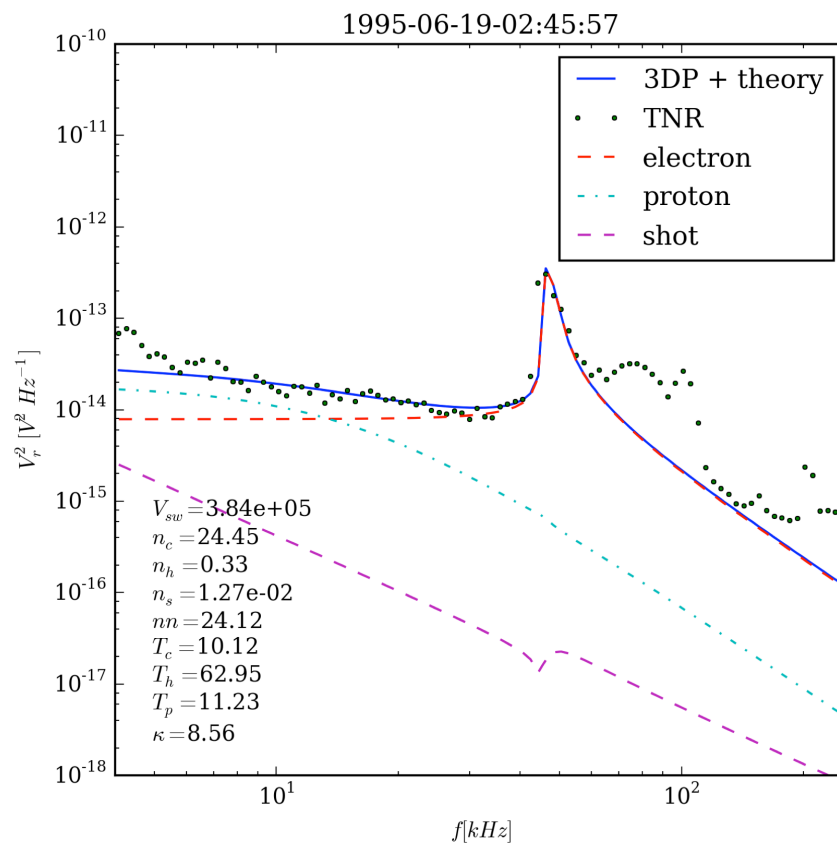
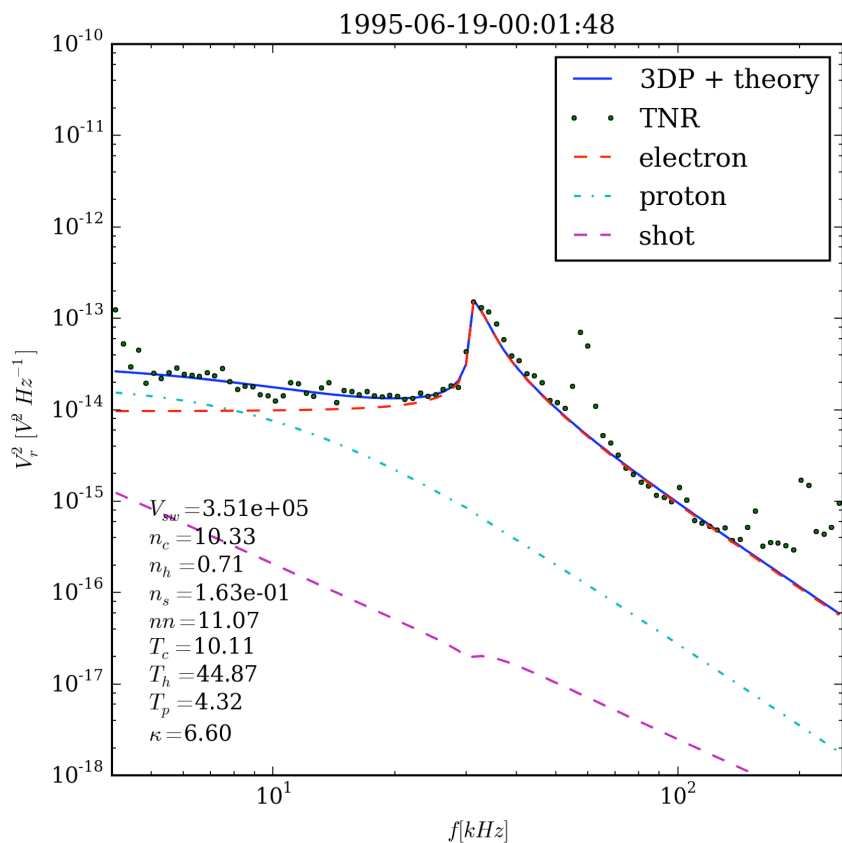


QTN: 2 Maxwellian vs Maxwellian+Kappa

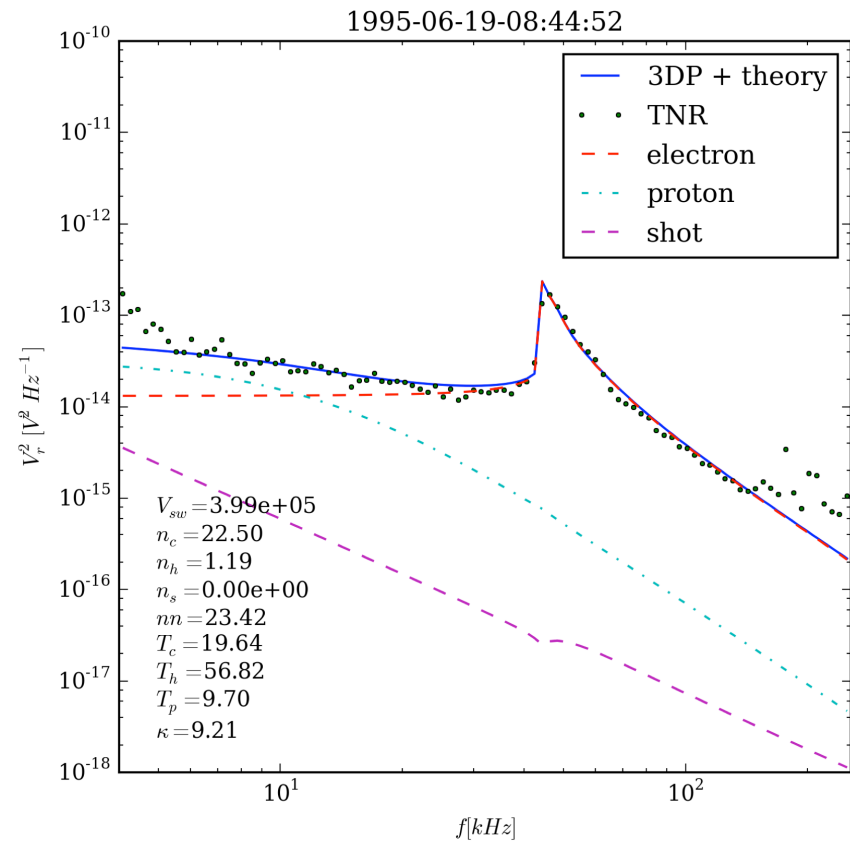
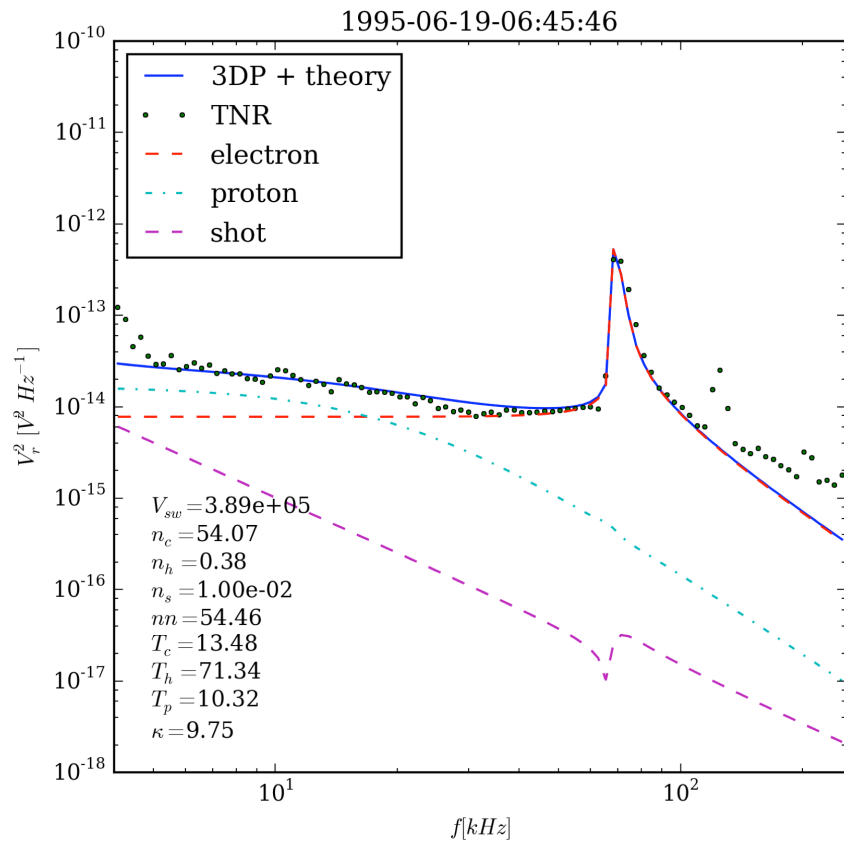


More examples of QTN with a Maxwellian + Kappa: using 3DP precision core+halo measurements

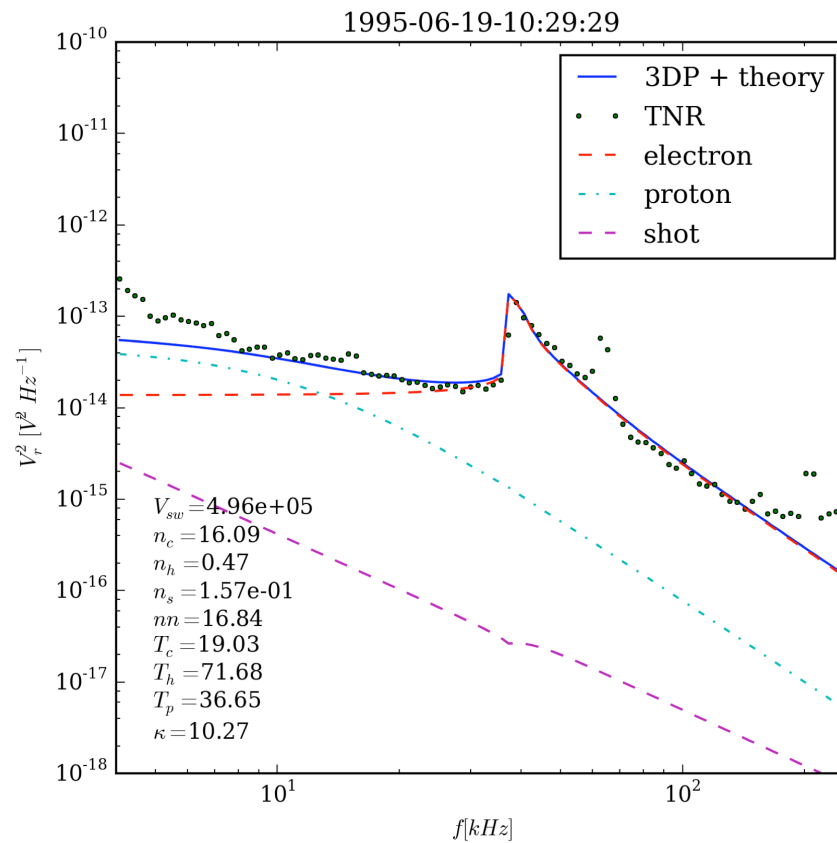
SLOW WIND examples



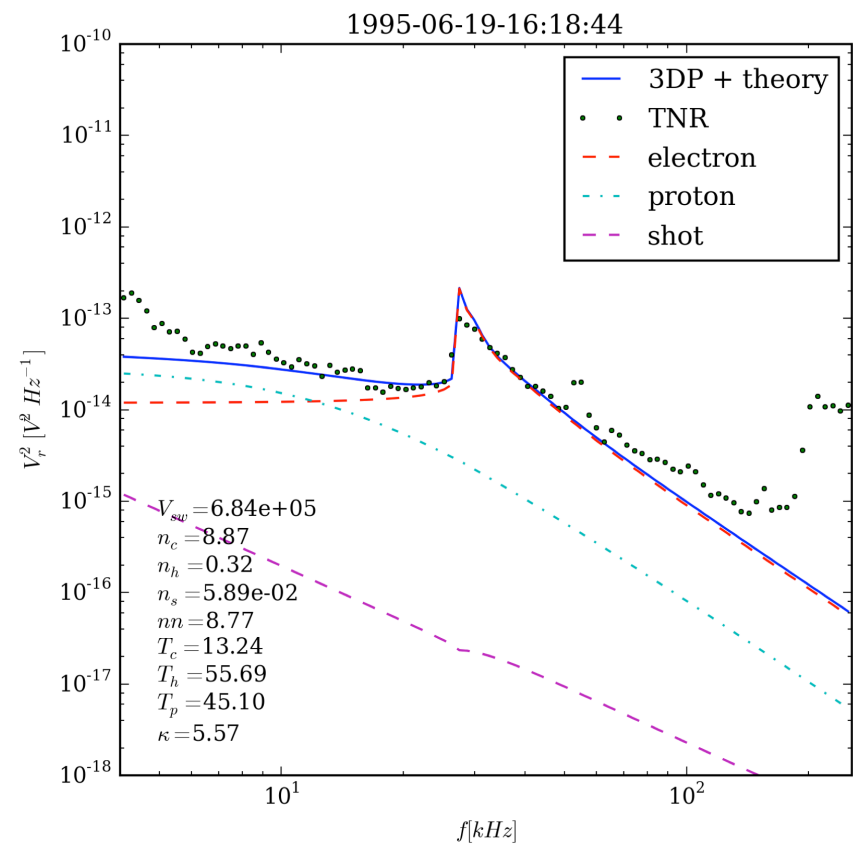
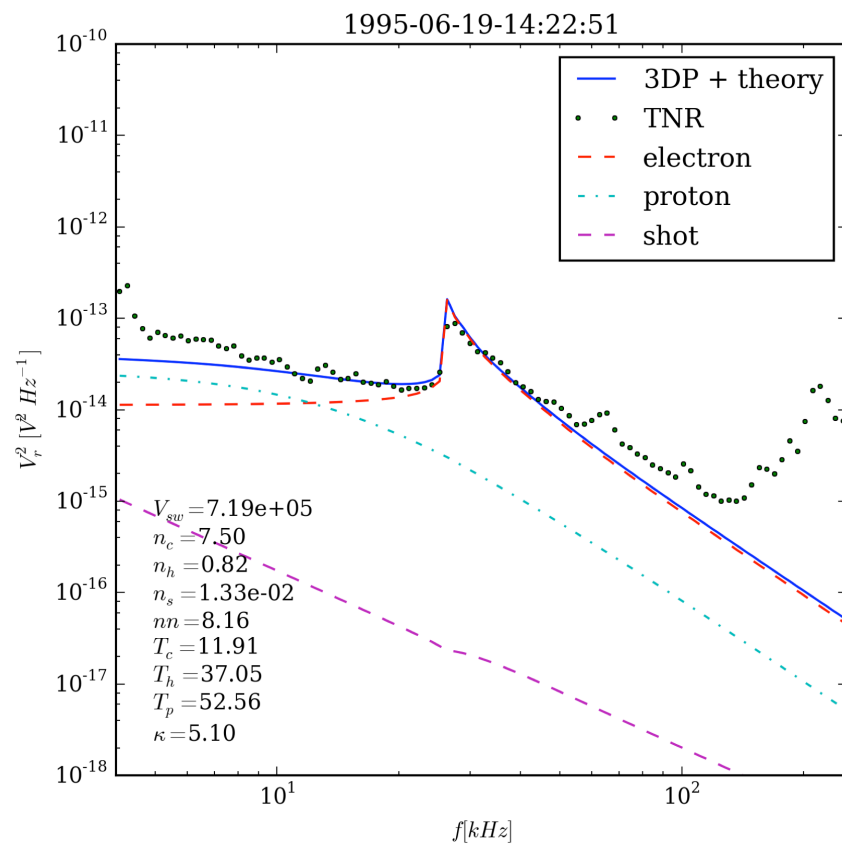
More slow wind examples



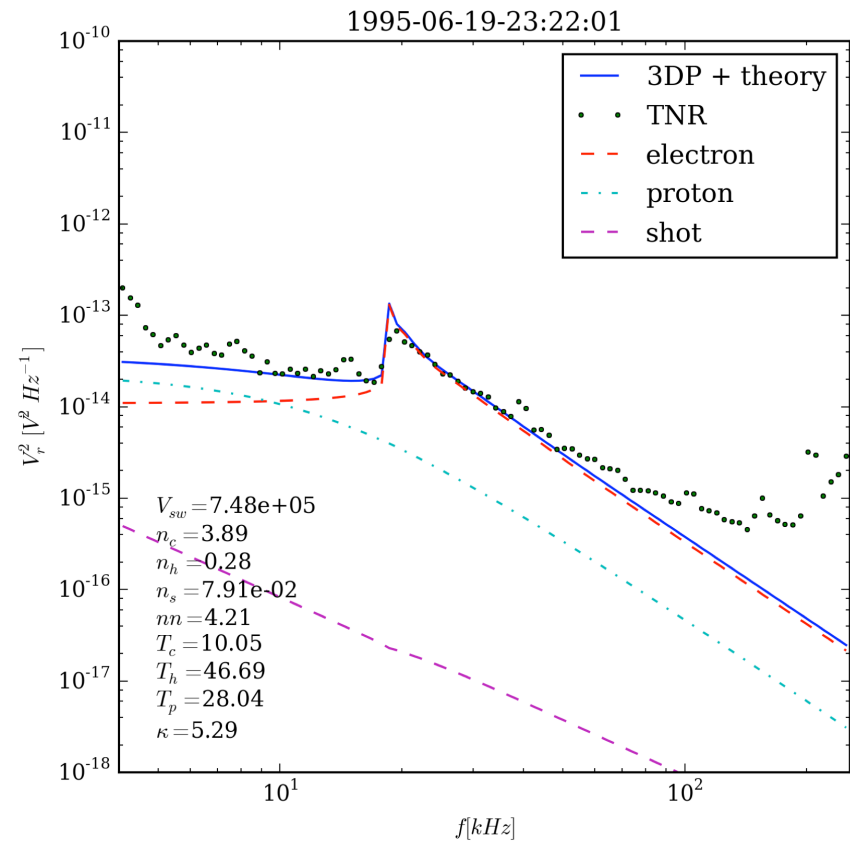
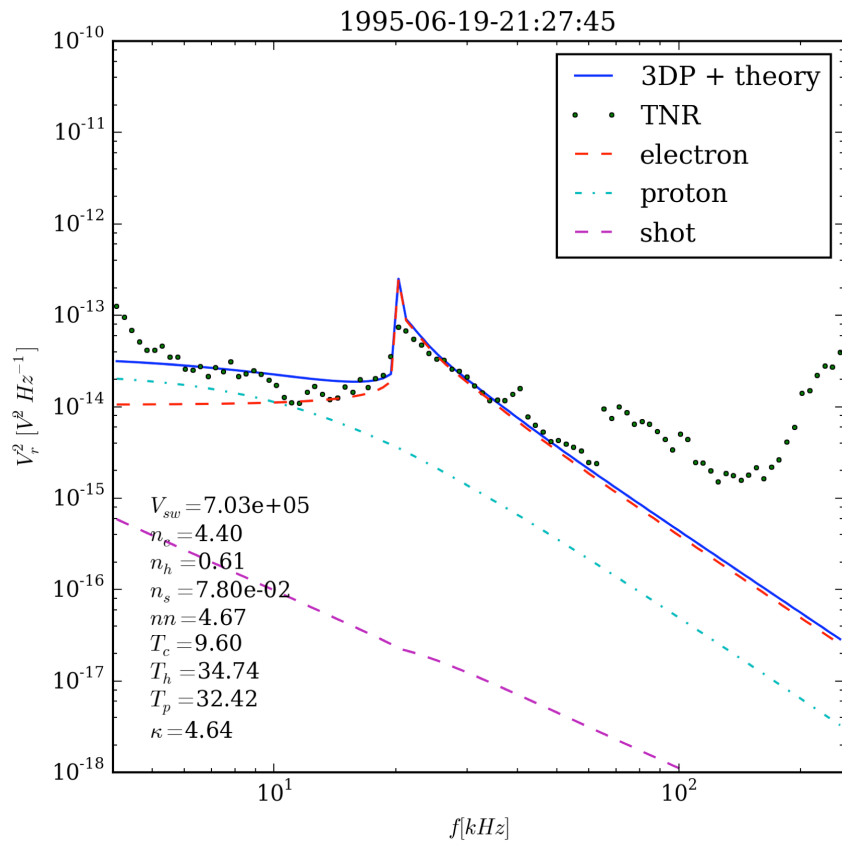
More slow wind examples



Fast wind examples



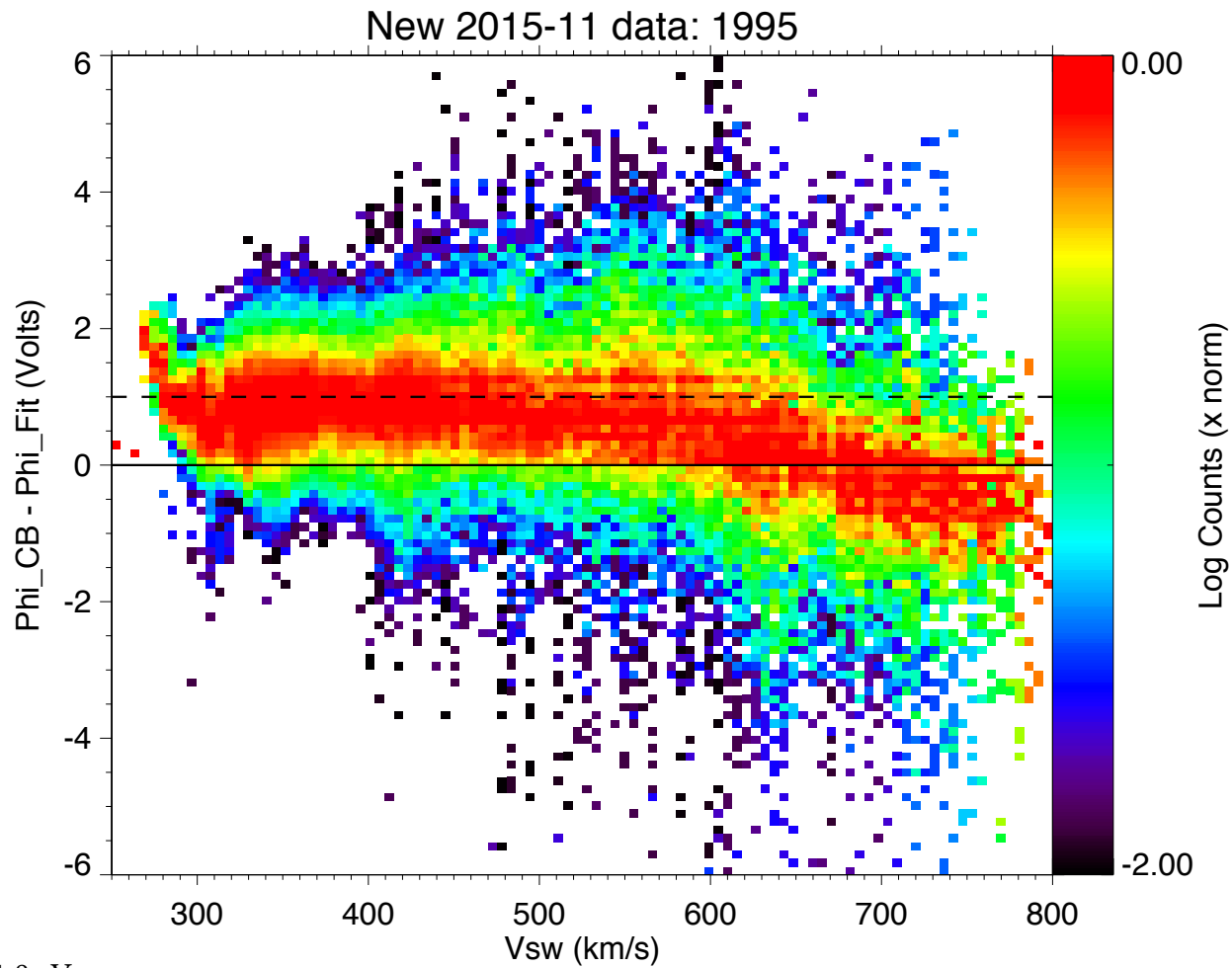
More Fast Wind examples



3DP electron database: Where are we at right now and what have we been working on lately?

- We have 4 years of validated data: 1995-1998.
- To produce more data beyond, we have to take into account and correct for the MCP efficiency for EESA-L at least. We have found that it starts affecting the counts.
- One effect is that the spacecraft potential determined by our fits differs for a given [Ne,Te] values at different years.
- So, we have been working on calibrating the “measured” s/c potential with a s/c potential determined by a current balance model between photoelectron, electron and ion currents that includes both thermal and bulk motions of solar wind ion and electrons. Both ion and electron VDFs are approximated by a single Maxwellian.

Differences between CB and Fit spacecraft potential



$T_{ph} = 1.8 \text{ eV}$
all regular currents: jph, je and ji

If the difference for $V_{sw} > 580\text{km/s}$ is due to the CB potential:

I included the following effects:

- Two isotropic populations of electrons: Core + Suprathermal (halo+strahl)
- Two photoelectron populations: a cold and a hot populations
- Effects on T_p uncertainties?
- Core and suprathermal drifts to the electron currents as these become important for high speed winds: the presence of the strahl forces the core to drift sunward at speeds of up to 180 km/s.
- Next is to estimate the current of secondary electrons as they can become significant in fast wind flows, and they'd contribute to increase the s/c potential, which is consistent with the previous plot.

If the difference for $V_{sw} > 580\text{km/s}$ is due to the Fit potential:

It could be that for the fast solar wind, the T_c is smaller and the strahl more pronounced, the core fit in the parallel direction could be more problematic, but the perpendicular fit should not be affected. => Thoughts: Fit potential less likely to be the culprit.

Estimating the detector/MCP efficiency to produce precision data further in the Wind mission

Hopefully, we will solve it shortly. We will then estimate the efficiency factor and determine a curve of Efficiency as a function of time, which we can use and apply to the measured counts before fitting the eVDFs.

$$f_c(v, t) = \zeta(t) \frac{N}{T^{3/2}} \exp(-v^2/2T) \exp(\phi/T)$$

True potential

$$f_c(v, t) = \frac{N}{T^{3/2}} \exp(-v^2/2T) \exp(\phi_0/T)$$

Potential that includes efficiency effects

$$\Rightarrow \phi = \phi_0 - T \log \zeta(t)$$

We tried this on one day of data in 1995 in the slow wind and we found:

$$\zeta \sim 0.97$$

Which is a good sign!!